

# Topology of the force network in the jamming transition of an isotropically compressed granular packing

Roberto Arévalo, Iker Zuriguel, and Diego Maza

*Departamento de Física, Facultad de Ciencias, Universidad de Navarra, E-31080 Pamplona, Spain*

(Received 27 November 2009; revised manuscript received 17 March 2010; published 14 April 2010)

The jamming transition of an isotropically compressed granular packing is studied by means of molecular dynamics simulations. The system is shown to undergo a critical transition which is analyzed by looking at the topological structure of the force network. At the critical packing fraction there is a sudden growth of the number of polygons in the network. Above the critical packing fraction the number of triangles keeps growing while the number of the rest of polygons is weakly reduced. Then, we prove that in the jammed regime, there is a linear relationship between the number of triangles and the coordination number. Furthermore, the presence of these minimal structures is revealed to be connected with the evolution of some important topological properties, suggesting its importance to understand the physical properties of the packing and the onset of rigidity during the compression.

DOI: [10.1103/PhysRevE.81.041302](https://doi.org/10.1103/PhysRevE.81.041302)

PACS number(s): 45.70.Vn

## I. INTRODUCTION

Any loose granular system isotropically compressed undergoes a transition from a dynamic state to another “arrested” or “frozen” characterized by its ability to resist different kinds of stresses. The nature of this transition has been profusely analyzed by many authors under different points of view and has received different names such as *percolating rigidity transition* or *jamming transition* along the last decades [1,2]. In all the cases a variety of restrictions and approximations have been included to analyze the critical origin of this transition. Nowadays it is widely accepted that when the packing fraction ( $\phi$ ) of the system reaches a critical value  $\phi_c$ , the coordination number,  $Z$ , coincides with the isostatic limit which depends on the existence of friction and the space dimensionality. Beyond the transition, the growth of  $Z$  is intimately related with the complex force distribution inside the packing [3–6].

Recently, Majmudar *et al.* [7] have demonstrated experimentally that an isotropically compressed granular system undergoes this type of transition. In the experiment, a bidimensional system of bidisperse disks in a stress-free state is compressed and subsequently decompressed until another essentially stress-free state is reached. The disks were photoelastic, allowing a precise determination of the contact points. The critical packing fraction was roughly calculated from the point where the pressure started to grow. Hence, the coordination number could be fitted by the power law  $Z - Z_c \propto (\phi - \phi_c)^\beta$ , where  $\beta \approx 0.5$  and  $Z_c = 3.04$ . This result was in excellent accord with previous simulations [8,9].

Other authors [4] also propose that the development of a peak in the force distribution is a signature of jamming, arguing that it is a consequence of the apparition of yield stress within the sample. Alternatively, variables such as the bulk modulus or the density of vibrational states have been used to describe the jamming transition for both frictionless [10] and frictional particles [11]. Makse *et al.* [5] have shown that this transition is characterized by a change on the granular force distribution: the distribution of forces corresponding to samples weakly compressed decays exponentially and

crosses over to a Gaussian when the packing fraction is increased above the critical value. Near the critical density, the development of linear “force chains” percolating the simulation box was observed along the compression direction. Hence, force chains were assumed to be responsible for the rigidity attained in the final solid state.

Recently, Ostojic *et al.* have proposed a new universality class for isotropically compressed granular media [12]. The authors built force networks by considering only forces above a varying threshold. Their main finding was that, independently of the system size or the packing parameters, the second moment of the cluster size distribution can be fitted by an universal function of a critical force threshold,  $f_c$ , and the system size (measured in terms of the total number of contacts  $N$ ). Although the scaling exponents are universal, the threshold  $f_c$  depends on the preparation conditions and its value is typically slightly larger than the average force of the packing.

A great advantage of the method used in [12] is that it examines the properties of the force network without referring to the widely used concept of “force chains.” An important problem of working with force chains is that there is not a clear definition [13], and its interpretation may vary from one author to another. Following the idea of Ostojic *et al.* [12] in this work we carry out a structural analysis of the force network of granular packing resorting to the tools used in *complex networks* [14,15]. Assuming that every grain with at least one contact is a *node* and the forces among grains are the *links* or *edges*, a graph can be defined for every granular system and its topology quantitatively characterized. Other authors have recently shown the usefulness of these tools to analyze the granular packing structure [16–18].

In this work we numerically study the force network evolution of isotropically compressed granular materials. In Sec. II the molecular dynamics simulations and the compression protocol are described in detail showing that the system undergoes a jamming transition. Then, in Sec. III, the evolution of the packing during the compression process is described by looking at several aspects of the contact network topology. Section IV is devoted to characterize the final highly

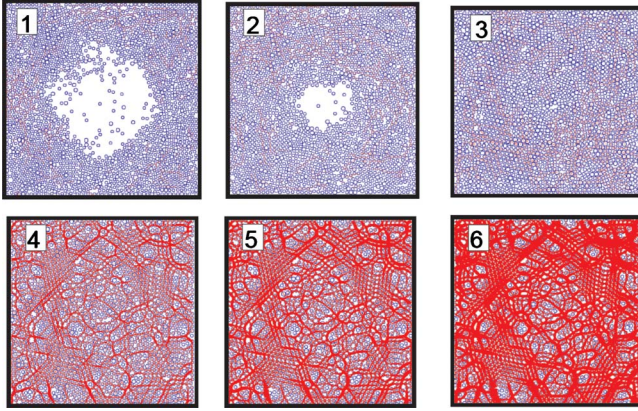


FIG. 1. (Color online) Evolution of the granular packing during the compression process for  $\phi=0.596$  (Fig. 1),  $\phi=0.741$  (Fig. 2),  $\phi=0.829$  (Fig. 3),  $\phi_c=0.838$  (Fig. 4),  $\phi=0.843$  (Fig. 5), and  $\phi=0.849$  (Fig. 6). The magnitudes of the normal forces are proportional to the widths of the chains.

packed configuration, evidencing the correlations between force magnitudes and topology. Finally, in Sec. V the results are summarized and discussed.

## II. NUMERICAL METHOD AND COMPRESSION PROTOCOL

We perform soft particle molecular dynamics simulations of the isotropic compression of disks in two dimensions. The granular sample consists on 307 disks of radii  $R_1=D/2$ , and 1741 disks of radii  $R_2=(7/9)R_1$ . Hence, the total number of particles is  $N=2048$ . Each simulation starts by setting the particles in a horizontal setup with random velocities (drawn from a Gaussian distribution) and random positions in a wide area such that no grain is in contact with any other. The packing fraction at this initial state is around 0.1. The interaction between disks is through normal and tangential forces as defined in [19]. The values used for the parameters of the force model are:  $\mu=0.5$ ,  $k_n=10^5$ ,  $\gamma_n=150$ ,  $k_s=\frac{2}{7}k_n$ , and  $\gamma_s=300$  with an integration time step  $\tau=10^{-4}\sqrt{D/g}$ . The stiffness constants  $k$  are measured in units of  $mg/D$ , the damping constants  $\gamma$  in  $m\sqrt{g/D}$ , where  $m$ ,  $D$ , and  $g$  stand, respec-

tively, for the mass of the disks, the diameter of the disks and the acceleration of gravity. This numerical method has been shown to reproduce experimental results of granular flows [20] and deposits of particles under the action of gravity [21].

The test cell consists of four moving walls, composed of the aforementioned disks, that compress the granular sample isotropically (Fig. 1). The compression is kept by applying a force  $F_w$  to the walls that increases by  $0.015mg$  every  $10^3$  time steps. The displacement of the walls is determined, through the equations of motion, by the total force on the walls which is the sum of  $F_w$  and the force that the grains exert on the walls. The simulations run until a packing fraction  $\phi\approx 0.90$  is reached. Twenty independent simulations were carried out yielding essentially the same results. Other simulations have been carried out modifying some properties such as the system size, the size distribution of the particles, the coefficient of friction, the maximum compression and the geometry of the cell. The dependence of the results on these parameters was proved to be very small [22].

It is important to remark that this compression protocol does not include annealing as most of the works reported in the literature do [6–10]. Hence, the jamming transition does not take place from a zero temperature state or point “J” where there is not any contact among the particles. This fact can be readily observable from Fig. 2(a) where  $Z$ , the average coordination number, is represented as function of the packing fraction  $\phi$ . During the whole compression process  $Z$  takes values around 1.5, displaying a sudden jump for  $\phi$  around 0.84. By analogy with the works that include annealing, the sudden increase of  $Z$  is an indication of the transition to a rigid state (see also the 5th and the 6th packing of Fig. 1).

In order to identify the exact point at which the jamming transition occurs, we examine the evolution of the average overlap per particle  $\delta$  [Fig. 2(b)]. Before the jamming, the average overlap is almost zero as the particles are in a dynamic state, weakly contacting each other. After the jamming, this magnitude grows linearly, and hence the value of  $\phi$  at which the average overlap starts to grow can be calculated. Analogously to the jamming transition at the J point, the value of  $\phi$  at which the average overlap starts to grow will be taken as the critical packing fraction,  $\phi_c$ . For each

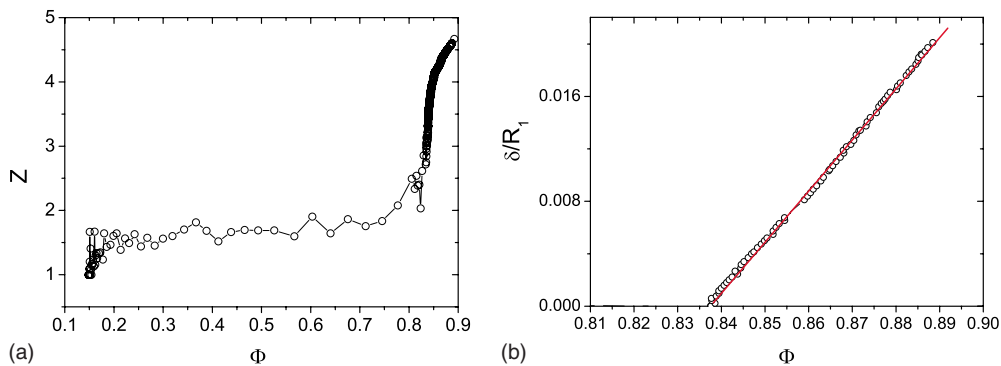


FIG. 2. (Color online) (a) Coordination number versus the packing fraction ( $\phi$ ) along the whole compaction process. The coordination number is calculated without taking into account rattlers, particles without contacts. (b) Average deformation ( $\delta$ ) rescaled with the radius of the greater disks ( $R_1$ ) versus the packing fraction. The continuous line is a linear fit.

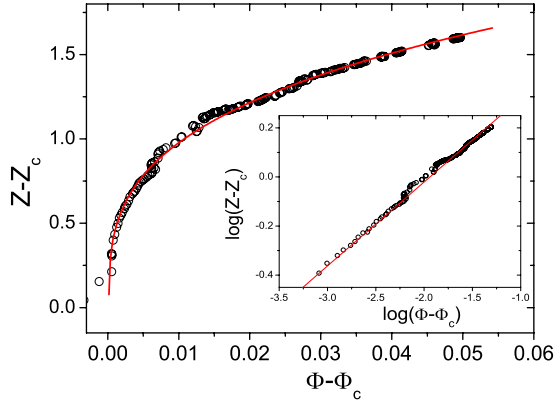


FIG. 3. (Color online) Excess coordination number versus the packing fraction above the critical point. The continuous line is a fit to  $Z-Z_c \propto (\phi-\phi_c)^\beta$  with  $\beta=0.33$ ,  $\phi_c=0.838$ , and  $Z_c=3.00$ . The inset shows the same results in logarithmic scale.

simulation run, a slightly different value for the critical packing fraction is obtained.

Once the transition is identified, the value of  $Z$  at this point,  $Z_c$ , is determined. Then, for each simulation, the excess of coordination number  $Z-Z_c$  is fitted as a function of the distance to the transition point  $(\phi-\phi_c)$ . All the simulations display the same functionality:  $Z-Z_c \propto (\phi-\phi_c)^\beta$  with  $\beta \approx 0.33$ . This result qualitatively resembles the one obtained with compression protocols that include annealing, though the value of the exponent  $\beta$  is significantly smaller [6–10]. The figures obtained for  $Z_c$  and  $\phi_c$  display a small dispersion but in all the cases lie close to  $\phi_c=0.838$  and  $Z_c=3$  which are the values of the fit shown in Fig. 3. It is important to remark that the coordination number is computed ignoring rattlers and that the values of the exponents depend strongly on  $Z_c$  and  $\phi_c$  like in jamming experiments at zero stress (see Ref. [10] of the work of Majmudar *et al.* [7]).

The transition displayed when the particles are isotropically compressed was previously analyzed by looking the force distribution [ $P(F)/\langle F \rangle$ ] evolution at different time steps during the compression [23]. In good agreement with [5,4], the force distribution decreases monotonically before the transition to rigidity and develops a peak beyond the time at which the average kinetic energy of the system suddenly decays.

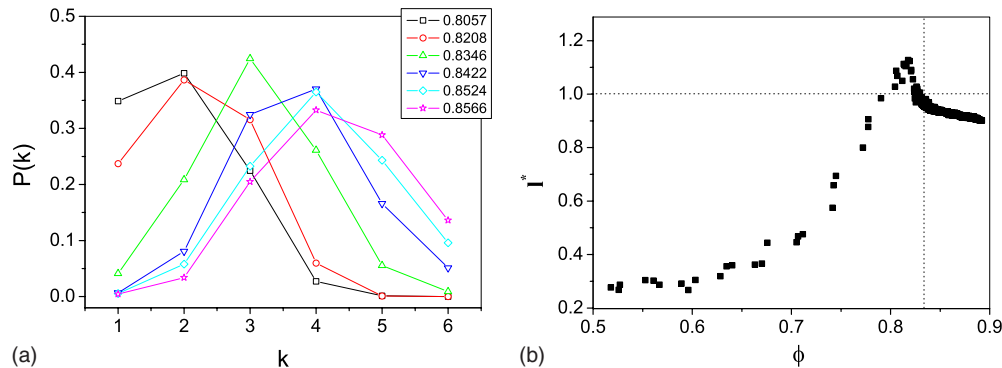


FIG. 4. (Color online) (a) Distribution of connectivities obtained for different values of  $\phi$  as indicated in the legend. (b)  $l^*$ , the average shortest path length normalized by  $\sqrt{N}/2$  versus the packing fraction  $\phi$ . The dotted lines indicate  $l^*=1$  and  $\phi=\phi_c$ .

### III. EVOLUTION OF THE CONTACT NETWORK TOPOLOGY

In order to investigate the jamming transition and more specifically, the structural origin of the excess of coordination number, we analyze the topology of the contact network during the compression. As mentioned before, any granular ensemble can be seen as a complex network formed by a set of nodes—any disk with at least one contact—and links corresponding to the contacts between disks. Two of the several magnitudes which are commonly used in the framework of complex networks to analyze these graphs are: (a) the connectivity,  $k$ , of a node which is simply the number of links connected to it and (b) the shortest path length,  $l$ , which is the longitude—measured in number of links—of the shortest path connecting two given nodes. The average shortest path between all the nodes of the network  $\langle l \rangle$  is a magnitude that characterizes the typical size of the network. Finally, we will also study the existence of closed topological structures or “polygons” formed by the links of the network. These can be defined as closed loops with the same initial and final nodes, formed by three, four or more steps, which we will simply term triangles, squares and so on. It is important to indicate that a condition for a polygon to be considered is that it does not contain interior links or smaller polygons. In other words, the polygons considered here surround empty spaces. The analysis of the polygons developed in the contact network has been recently shown to reveal important information about the stability of tilted granular samples [16] and dense granular materials under quasistatic biaxial loading [17].

In Fig. 4(a) the distribution of connectivities  $P(k)$  for a typical run is plotted for different values of the packing fraction. For values of  $\phi$  below  $\phi_c$  the distribution shows a maximum at  $k=2$  indicating the predominance of linear or filamentary structures. Around  $\phi_c$  the maximum shifts to three, and for increasing densities moves to higher values as a consequence of the development of a highly connected network. In Fig. 4(b) the values of  $l^*$  (the average shortest path length  $\langle l \rangle$  normalized by  $\sqrt{N}/2$ ) are displayed as a function of the packing fraction. For small packing fractions,  $l^*$  is low as the network is composed of small isolated clusters of connected particles. When  $\phi$  is increased, nodes and links are added with the consequent increase of  $l^*$ . Before  $\phi_c$  [dotted line in



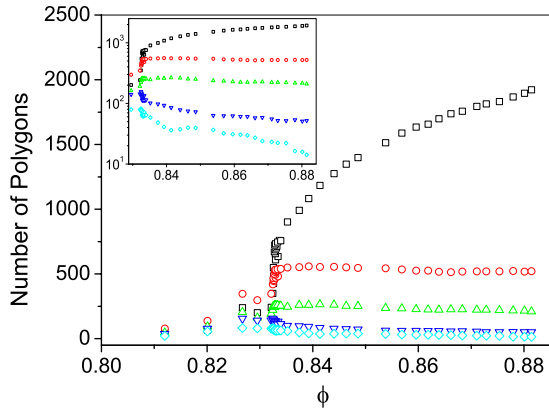


FIG. 5. (Color online) Number of the different polygons versus  $\phi$ . Inset: the same data in semilogarithmic scale. Different symbols are used for triangles ( $\square$ ), squares ( $\circ$ ), pentagons ( $\triangle$ ), hexagons ( $\nabla$ ) and heptagons ( $\diamond$ ). Triangles are the only polygons which grow in number after the transition.

Fig. 4(b)] the average shortest path reaches a maximum indicating the existence of chains connecting opposite sides of the system that is still in an unjammed state. After the maximum,  $l^*$  quickly decreases suggesting the formation of new links that shorten the distance between nodes that were already present in the network. It is interesting to note that  $l^*$  takes a value of approximately one for the critical density. Above  $\phi_c$  the average shortest path keeps decreasing as new links form in the jammed sample.

#### Polygons in the contact network

As mentioned above, the fact that  $l^*$  decreases before the jamming transition suggests the development of links shortening the distance between nodes that were already connected at smaller values of  $\phi$ . This would imply the apparition of closed loops (polygons) within the network near the transition point. In Fig. 5 we present the number of polygons formed of three to seven nodes for different values of  $\phi$ . The first result that becomes apparent is that at low packing fractions there are only a few (nonstationary) polygons which indicates that the contact network is mainly linear. When the packing fraction approaches  $\phi_c$  a sudden jump is observed in the number of polygons. Remarkably, beyond  $\phi_c$  the number of triangles keeps growing whereas the number of other polygons gently decreases. There is not a clear relationship between the growth rate of triangles and the reduction rate of other polygons. Nevertheless, it is clear that the increment in the number of triangles (NT) should be related with the coordination number above  $\phi_c$ . Indeed, the relationship between NT and  $\phi$  resembles the growth of  $Z$  with  $\phi$  displayed in Fig. 2(b).

In Fig. 6 the number of triangles  $NT$  is displayed as a function of the coordination number  $Z$ . Interestingly, no dispersion is found in the transition for the different simulations, suggesting that both magnitudes are strongly related. While the dependence of  $NT$  with  $Z$  is nonlinear near the transition point [23], the asymptotic dependence seems to be linear. This linearity indicates that, once the system is above

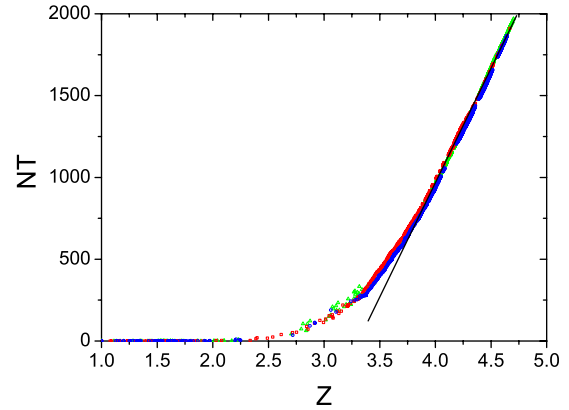


FIG. 6. (Color online) Number of triangles (NT) vs  $Z$ . Different symbols are used for three typical runs. The continuous line is a fit of the asymptotic linear dependence.

the critical packing fraction, there is a constant probability of creating a new triangle when a link is added to the network. A direct consequence of the proportionality of  $NT$  with  $Z$  is that  $NT$  versus  $\phi$  could be fitted using the same law than the used for the excess of coordination number.

#### IV. FORCE TOPOLOGY IN THE HIGHLY PACKED STATE

In the previous section we showed the importance of the polygonal structures (in particular triangles) to understand the critical nature of variables such as the coordination number. In this section we will analyze the role that these structures play in the force transmission within the sample. For this reason we will focus on a highly packed state, with a value of  $\phi=0.892$  which is considerably above  $\phi_c$ . In order to characterize the forces inside the packing we introduce a parameter  $f=F_{th}/\langle F \rangle$ , where  $\langle F \rangle$  is the average force in each sample. Accordingly, the nodes of the network will be the particles with at least one contact with a normal force above  $F_{th}$ . Note that the force network built with  $f=0$  includes all the contacts and hence coincides with the contact network used in the previous section. On the other hand, tuning  $f$  to values larger than zero, we obtain *diluted* graphs with varying behavior of its topological properties. Indeed, when the parameter  $f$  is increased, the network disaggregates giving rise to the formation of clusters: groups of nodes which are mutually linked but are disconnected from other groups ( $f=1.5$  in Fig. 7). In previous works, the use of these force networks has been proved to be useful to understand several properties of granular materials [12,22,23].

As can be seen in Fig. 7 the force networks obtained for different values of  $f$  display completely dissimilar properties: for small values of  $f$  the force network presents polygonal structures whereas it is predominantly linear for  $f>1$ . Then, it can be said that polygonal structures disappear when only high forces are considered. This result is clearly shown in Fig. 8 where the number of polygons is computed as a function of  $f$ : the number of closed loops is almost zero when forces larger than the average are considered. This indicates that the majority of the polygons contain *at least one contact carrying a weak force*. In addition, the inset of Fig. 8 reveals

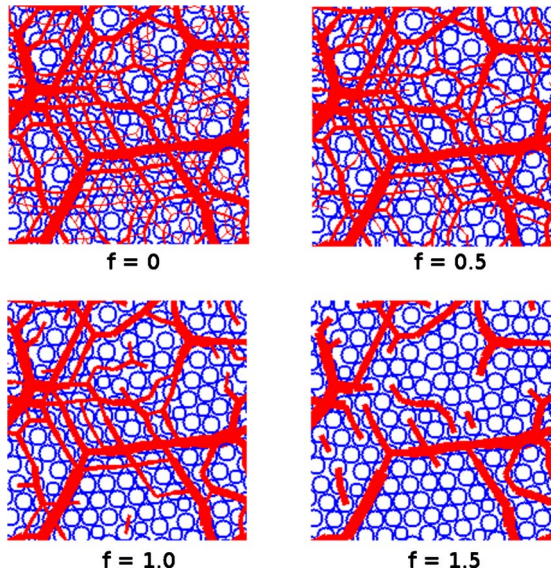


FIG. 7. (Color online) A region of a compressed packing ( $\phi = 0.892$ ) showing the effect on the network of taking several values of the parameter  $f$ .

that the number of all polygonal structures decays exponentially as  $f$  is increased beyond one. In the region going from  $f=0$  to  $f=1$  triangles present distinct behavior as they are the only polygonal structure which number decreases. The number of the other polygons remains fairly constant or slightly increases. We speculate that this augment in the number of high order polygons is a consequence of the reduction in the number of triangles. It sounds plausible that a triangle that disappears due to the elimination of one of its edges gives rise to the apparition of a higher order polygon.

An alternative way to characterize the polygonal structure is through the clustering coefficient  $C$  of the graph [24]. For a given node  $i$ , the clustering coefficient  $c_i$  is calculated as  $c_i = e_i / [k_i(k_i - 1) / 2]$  where  $k_i$  is the number of nodes connected to  $i$ ,  $k_i(k_i - 1) / 2$  the maximum number of connections among those  $k_i$  nodes, and  $e_i$  the actual number of connections among the  $k_i$  nodes connected to the particle  $i$ . In other

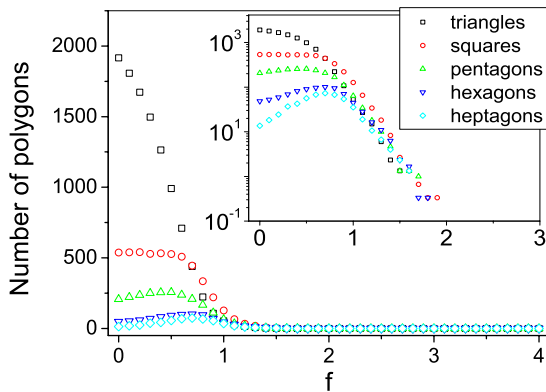


FIG. 8. (Color online) Number of polygons in a highly packed configuration ( $\phi=0.892$ ) as a function of the parameter  $f$ . The inset shows the same data in semilogarithmic scale. The legend indicates the symbols used for triangles, squares, pentagons, hexagons, and heptagons.

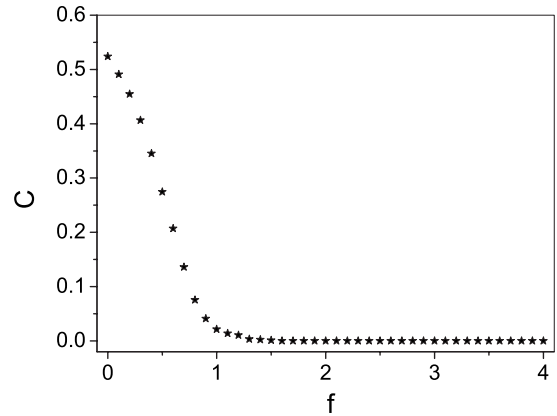


FIG. 9. Clustering coefficient as a function of the parameter  $f$  for the same highly packed configuration than the one presented in Fig. 8.

words,  $e_i$  is the number of third order loops that the node  $i$  belongs to. The clustering coefficient of the network  $C$  is calculated as the average of the clustering coefficient of the individual nodes. Hence, it sounds reasonable that the trend displayed by the clustering coefficient  $C$  versus the force threshold  $f$  (Fig. 9) resembles the one obtained for the number of triangles (Fig. 8).

Additional evidence of the filamentary character of the force networks obtained with  $f > 1$  and the polygonal nature of the force networks obtained with  $f < 1$  can be gained by looking at the number of nodes ( $n_p$ ) and the number of contacts ( $n_c$ ) in the diluted networks. As a linear chain of  $n_p$  grains has  $n_p - 1$  contacts, a completely filamentary network formed by one cluster without ramifications must obey  $n_c - n_p + 1 = 0$ . Hence, from now on we will refer to  $n_c - n_p + 1$  as the *excess of contacts* EC. Values of  $EC > 0$  indicate the existence of ramifications in the network whereas values of  $EC < 0$  suggest the existence of several filamentary clusters [25]. In Fig. 10 the *excess of contacts* is represented as a function of  $f$  for a highly packed state. As it is expected, for values of  $f$  close to zero, the contact network is an intricate structure with a high number of contacts per particle. When  $f$  is increased, EC rapidly decreases reaching negative values for  $f$  slightly above one. For these  $f$  values, the network is mainly formed by several filamentary clusters as displayed in

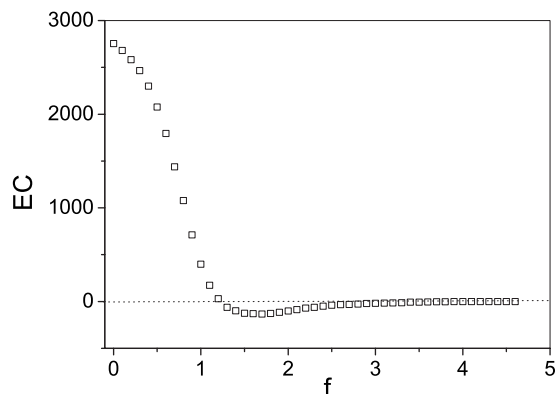


FIG. 10. The *excess of contacts* EC obtained for a packing of  $\phi=0.892$  as a function of the parameter  $f$ .

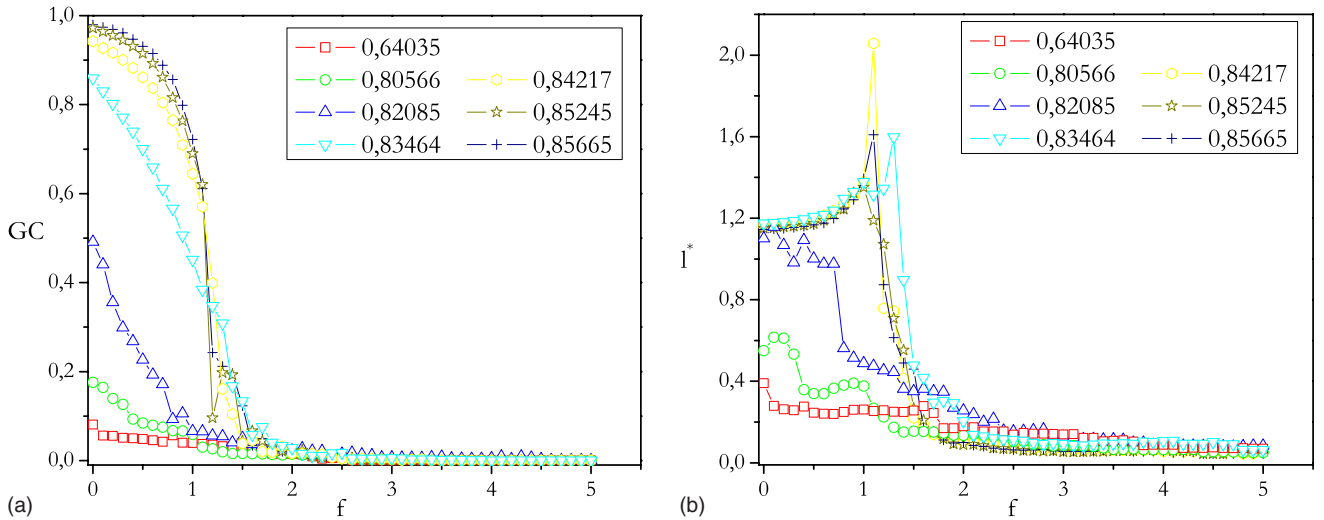


FIG. 11. (Color online) (a) Size of the giant component in the network (GC) resulting after applying distinct values of the force threshold  $f$ . GC is given in number of grains and normalized with the total number of grains in the sample ( $N$ ). (b) Average shortest path length normalized by  $\sqrt{N}/2$  for values of  $f$  going from 0 to 5. In both figures different symbols are used for different packing fractions as indicated in the legends.

Fig. 7 for  $f=1.5$ . For very high values of  $f$  the *excess of contacts* smoothly grows and tends to zero as the number of clusters in the network is reduced.

## V. DISCUSSION

In this work we have studied a bidimensional system of frictional grains isotropically compressed. Although the compression protocol does not include annealing we have shown that the system undergoes a transition that resembles the one resulting from the zero temperature case. Subsequently, we have analyzed several topological properties of the contact network and their evolution during the compression. This allowed us to find that the transition to a rigid state can be characterized by the development of a polygonal structure dominated by triangles which seems to give stability to the previously formed filamentary structure.

The force network in a highly compressed packing is analyzed using the threshold parameter  $f$ . This study suggests that the filamentary structure mainly carries large forces whereas the polygonal structure allocates most of the weak. This result is in agreement with the idea presented by Radjai *et al.* [26] who proposed that the network of contacts of granular packing is composed of two subnetworks, one “weak” formed by links carrying forces smaller than the average and another “strong” constituted by links carrying forces above the average. In order to prove the validity of this scenario we have analyzed the evolution of the force networks obtained for different  $f$  as the system undergoes the transition to rigidity. In Fig. 11 we present results of two topological indicators of these networks: the average shortest path length (that was already used for the contact network) and the giant component GC which is the number of nodes of the largest cluster in the network.

The giant component displays similar qualitative behavior for all the states with packing fraction above  $\phi_c$  [Fig. 11(a)].

When  $f$  is increased from  $f=0$  to  $f=1$  and small forces are removed from the network, the size of the GC decreases very slowly. After  $f=1$  the size of the giant cluster decays abruptly, being vanishing small for  $f \gtrsim 1.5$ . This behavior can be understood if we remind that the small forces belong to the polygonal structure. Hence, removing links belonging to polygons does not affect to the size of the giant component since their nodes remain connected through other links. Only a small reduction in GC is obtained due to the disconnection of single nodes. Above  $f=1$  the elimination of links causes a decrease in size of the giant component as the remaining structure starts to disaggregate. For packing fractions below  $\phi_c$  the resulting curves display qualitatively different behavior as in these states the polygonal structure has not been developed yet. Consequently the region for small values of  $f$ —where the reduction in GC is very weak—is not observed.

In Fig. 11(b) it is shown the average shortest path length  $l^*$  obtained for different values of the force threshold in states with different  $\phi$ . For densities above the critical,  $l^*$  displays a peak in the vicinity of the average force which is a result of the polygonal nature of the weak network, as explained in Sec. IV. For packing fractions below  $\phi_c$ , the peak in  $l^*$  is not observed as the polygonal structure is not developed. Hence, when  $f$  is reduced from 1 to 0, shortcuts between already connected nodes do not appear and  $l^*$  does not decrease. Let us mention that in jammed states, the peak in  $l^*$  is presented for values of force slightly larger than the average force. The fact that the values obtained for the critical force in [12] were similar suggests that both magnitudes could be related.

Interestingly, the features displayed by GC and  $l^*$  suggest the possibility to analyze the evolution of the final force network as a case of continuous percolation [27] where the contact topology is determined by  $f$ . Accordingly, we found that the value of  $f$  where the system percolates (allowing the connection between opposite sides of the packing) is around  $f=1.2$  coinciding with the value of  $f$  where the giant com-

ponent of the network GC decreases abruptly and  $l^*$  displays a peak. Therefore, a continuous percolation approach could provide information about the suitable scaling relationships to analyze this transition.

From the results of GC and  $l^*$  we confirm that the force network of an isotropically compressed sample is formed by two subnetworks: a strong one that is filamentary and develops before the transition to the rigid state and a weak one, which is mainly polygonal and develops just in the transition to rigidity. Additionally, the results reported in this work suggest that polygons—and triangles in particular—play a special role in the transition to the rigid state. Indeed, it can be argued that triangles are the mechanical structures that give rigidity to the network. This idea is in excellent agreement with the work of Tordesillas *et al.* [17] which has been recently published. In this work it is proved that triangles are important to understand the behavior of a dense granular material under quasistatic biaxial loading. In addition it is shown that these topological structures provide a dual resistance to force chain buckling both by providing strong lateral support to the force chains and by impeding rotation of the particles. In this sense, Rivier conceives a granular medium

as a set of nodes (grains) connected by rigid bars if they are in contact [28]. If it is assumed that the grains in contact roll without slip, the contact points can be considered as flexible hinges. In a circuit formed by an even number of disks or spheres all the components can rotate. Thus, a packing with only even circuits is unable to resist any shear stress as there is no frustration in the rotations. Instead, odd circuits frustrate rotations and this is a sufficient condition for the stability of the material. Despite slip among particles is allowed in our system, we have proved that triangles (the minimal odd circuits) are key structures to understand the transition to rigidity.

#### ACKNOWLEDGMENTS

This work was supported by Project No. FIS2008-06034-C02-01 (MICINN, Spain) and PIUNA (University of Navarra). R.A. thanks Asociación de Amigos de la Universidad de Navarra for support. The authors are grateful to S. Ardanza, A. Garcimartín, and L. A. Pugnaloni for helpful discussions concerning this work.

- 
- [1] C. F. Moukarzel, *Phys. Rev. Lett.* **81**, 1634 (1998).  
 [2] A. J. Liu and S. R. Nagel, *Nature (London)* **396**, 21 (1998).  
 [3] S. Henkes and B. Chakraborty, *Phys. Rev. Lett.* **95**, 198002 (2005).  
 [4] C. S. O'Hern, S. A. Langer, A. J. Liu, and S. R. Nagel, *Phys. Rev. Lett.* **86**, 111 (2001).  
 [5] H. A. Makse, D. L. Johnson, and L. M. Schwartz, *Phys. Rev. Lett.* **84**, 4160 (2000).  
 [6] H. P. Zhang and H. A. Makse, *Phys. Rev. E* **72**, 011301 (2005).  
 [7] T. S. Majmudar, M. Sperl, S. Luding, and R. P. Behringer, *Phys. Rev. Lett.* **98**, 058001 (2007).  
 [8] L. E. Silbert, D. Ertas, G. S. Grest, T. C. Halsey, and D. Levine, *Phys. Rev. E* **65**, 031304 (2002).  
 [9] C. S. O'Hern, S. A. Langer, A. J. Liu, and S. R. Nagel, *Phys. Rev. Lett.* **88**, 075507 (2002).  
 [10] C. S. O'Hern, L. E. Silbert, A. J. Liu, and S. R. Nagel, *Phys. Rev. E* **68**, 011306 (2003).  
 [11] E. Somfai, M. van Hecke, W. G. Ellenbroek, K. Shundyak and W. van Saarloos, *Phys. Rev. E* **75**, 020301(R) (2007).  
 [12] S. Ostojic, E. Somfai, and B. Nienhuis, *Nature (London)* **439**, 828 (2006).  
 [13] J. F. Peters, M. Muthuswamy, J. Wibowo, and A. Tordesillas, *Phys. Rev. E* **72**, 041307 (2005).  
 [14] L. F. Costa, F. A. Rodrigues, G. Travieso, and P. R. Villas Boas, *Adv. Phys.* **56**, 167 (2007).  
 [15] S. Boccaletti, V. Latora, Y. Moreno, M. Chavez, and D. U. Hwang, *Phys. Rep.* **424**, 175 (2006).  
 [16] A. G. Smart and J. M. Ottino, *Phys. Rev. E* **77**, 041307 (2008).  
 [17] A. Tordesillas, D. M. Walker, and Q. Lin, *Phys. Rev. E* **81**, 011302 (2010).  
 [18] D. M. Walker and A. Tordesillas, *Int. J. Solids Struct.* **47**, 624 (2010).  
 [19] R. Arévalo, D. Maza, and L. A. Pugnaloni, *Phys. Rev. E* **74**, 021303 (2006).  
 [20] C. Mankoc, A. Janda, R. Arévalo, J. M. Pastor, I. Zuriguel, A. Garcimartín, and D. Maza, *Granular Matter* **9**, 407 (2007).  
 [21] I. Zuriguel, T. Mullin, and R. Arévalo, *Phys. Rev. E* **77**, 061307 (2008).  
 [22] R. Arévalo, I. Zuriguel, and D. Maza, *Int. J. Bifurcation Chaos Appl. Sci. Eng.* **19**, 695 (2009).  
 [23] R. Arévalo, I. Zuriguel, S. A. Trevijano, and D. Maza, *Int. J. Bifurcation Chaos Appl. Sci. Eng.* **20** (2010).  
 [24] D. J. Watts and S. Strogatz, *Nature (London)* **393**, 440 (1998).  
 [25] As an example, in a *diluted* graph composed by three perfectly linear clusters the value of the *excess of contacts* will be  $EC = n_C - n_P + 1 = -2$ .  
 [26] F. Radjai, M. Jean, J. J. Moreau, and S. Roux, *Phys. Rev. Lett.* **77**, 274 (1996).  
 [27] I. Balberg, *Philos. Mag. B* **55**, 991 (1981).  
 [28] N. Rivier, *J. Non-Cryst. Solids* **352**, 4505 (2006).